The Short-Range Structure of Aluminophosphate Oxynitride Catalysts. An ab Initio and Experimental Study

Antonio Márquez,*,† Javier Fernández Sanz,† José J. Benítez,‡ Miguel A. Centeno,‡ and José Antonio Odriozola‡

Departamento de Química Física, Facultad de Química, Universidad de Sevilla, E-41012 Sevilla, Spain, and Departamento de Química Inorgánica e Instituto de Ciencia de Materiales de Sevilla, Centro Mixto Universidad de Sevilla-CSIC, PO Box 874, E-41080 Sevilla, Spain

Received: July 15, 1999; In Final Form: September 24, 1999

In this study we combine spectroscopic data (diffuse reflectance infrared Fourier transform spectroscopy, DRIFTS, and X-ray photoelectron spectroscopy, XPS) with ab initio SCF calculations on model systems in order to get insight into the short-range order of amorphous aluminophosphate oxynitride (AlPON) catalysts. The use of fixed P/Al = 1/1 atomic ratio and varying N/O atomic ratio in the models, allowed us to consider stoichiometries with nitrogen contents in the range 0−20 wt %, similar to those found experimentally. The observed trends in computed Koopman ionization potentials (IPs), vibrational frequencies, and thermodynamic stability are compared with experimental XPS and DRIFTS data and available information of aluminophosphate and related systems. They are used to propose a structural model for the short-range structure of amorphous aluminophosphate oxynitrides. From the XPS data it can be concluded that first nitrogen enters the phosphorus coordination sphere; this results in the formation step by step of $[PO_3N]$ and $[PO_2N_2]$ polyhedra that coexist with $[PO_4]$ ones, their relative proportion depending on the total nitrogen content of the sample. On the basis of both experimental and ab initio SCF calculations, it can be concluded that the amorphous solids are formed by P−X−P (X = O, N) rings connected to each other by aluminum atoms. On the basis of the thermodynamic stability of the different bonds, nitrogen enters preferentially the phosphorus coordination sphere.

1. Introduction

Microporous materials such as zeolites, aluminophosphates, and their transition metal substituted analogues are currently the subject of an intensive research effort. The application of highly sophisticated experimental techniques, in particular spectroscopic methods such as high-resolution solid-state magic angle spinning NMR (MAS-NMR) spectroscopy, X-ray photoelectron spectroscopy (XPS), and diffuse reflectance infrared Fourier transform spectroscopy (DRIFTS), among others, provides adequate experimental tools for characterizing solid structures at the atomic level. However, the interpretation of these experimental results is often difficult, and the structure−catalytic activity relationship is better understood in terms of model systems where the main features of the catalysts are retained. The inherent complexity of these heterogeneous catalytic systems suggests that useful progress should be possible by an adequate understanding of key aspects of such catalysts through experimental and theoretical studies of idealized model systems. Molecular models of solids are an adequate means of applying ab initio theoretical methods to understand solid-state problems.[1] However, the reliability of computational chemistry studies of solids is limited mainly by the reduced size of the models compared to the basically infinite nature of the solid framework, and by inherent approximations on the theoretical methods used. In spite of these limitations, an increasing number of ab initio quantum chemical studies of solid systems has been reported in the literature in recent years. The reason for this tremendous increase of interest in the theoretical description of the chemistry and physics of solids and their surfaces is connected to recent advances in materials science, catalysis, and solid-state chemistry and physics that are relevant to important technological fields. Electronic devices, selective catalysts, and advanced materials designed for specific needs are at the leading edge of these advances.

Amorphous aluminophosphates (AlPO) have been shown to be effective catalysts in a wide variety of processes[2−4] and as support for other catalytic systems such as oxides[5−7] or metals.[8] Recently it has been shown that by nitridation of amorphous AlPO, a new solid with enhanced basic properties (AlPON) can be obtained.[9,10] Aluminophosphate oxynitride (AlPON) solids have been successfully tested as efficient high-surface-area basic catalysts in the Knoevenagel condensation.[11−13] Later bifunctional metal-supported AlPON catalytic systems combining the features of supported metals such as their hydrogenating power and the basicity of the support have been employed in the synthesis of methyl isobutyl ketone (MIBK)[14] or isobutane dehydrogenation.[15,16] Surface basicity as well as thermal stability of AlPON and metal-supported AlPON catalysts have been thoroughly studied,[13,15−20] and conclusions have been drawn on the local structure of surface species.

Recently, we have shown that ab initio theoretical methods are adequate for describing the short-range structure of amorphous aluminophosphates[21] while obtaining information on the electronic structure and hence on the acid−base properties of the solids. Data on the local structure of this new family of solid-based catalysts are scarce, and in most cases only indirect evidence on the local structure is obtained. The presence of an intense band in the infrared spectrum around 1300 cm^{-1} in both

* Corresponding author. E-mail: marquez@cica.es.
† Universidad de Sevilla.
‡ Centro Mixto Universidad de Sevilla-CSIC.

10.1021/jp992413w CCC: $18.00
Published on Web 11/16/1999

AlPON and AlGaPON catalysts (see, e.g., refs 13, 15, 17, and 19) has been ascribed to the existence of P═O and/or P−N bonds and the evolution of the surface basicity and catalytic activity to a modification of the coordination polyhedra around phosphorus atoms. Also, the presence of several coordination polyhedra around phosphorus and aluminum has been inferred by MAS NMR spectroscopy.[22]

In this study we combine spectroscopic data with ab initio SCF calculations on model systems in order to get insight into the short-range order of amorphous AlPON catalysts. The observed trends in computed Koopman ionization potentials (IPs), vibrational frequencies, and thermodynamic stability are compared with experimental XPS and DRIFTS data and available information on aluminophosphate and related systems. This analysis is used to propose a structural model for the short-range structure of amorphous aluminophosphate oxynitrides.

2. Computational Details

Ab initio SCF calculations were undertaken using Dunning's double-ζ quality (9s,5p)/(3s,2p) basis set with polarization functions added on the heavy atoms. The use of d-type polarization functions on the heavy atoms is mandatory for the correct description of the bonding characteristics of these atoms. In particular, it is a prerequisite for the adequate description of the hypervalence of P atoms.

All geometries have been fully optimized at the RHF−SCF level by standard gradient techniques. The stationary points found were characterized as minima by fully analytical computation of the second derivatives of the energy in a Cartesian representation. In order to obtain a set of physically meaningful force constants, this matrix was transformed into an internal coordinate representation. To avoid redundancies in the internal coordinate set used, in particular for the eight-membered rings, internal symmetry-global coordinates were used, as described by Pulay et al.[23,24] The full description of the internal coordinates and the symmetry-global coordinates are available from the authors upon request.

Infrared (IR) intensities were computed by numerical differentiation with respect to an external homogenous electric field of the analytically computed forces. The procedure is fully described elsewhere.[25]

All the calculations were performed using a parallel version of the HONDO program[26−28] running on a HP X-Class SPP-2000 server and on a Digital AlphaServer computer.

3. Experimental Procedure

Aluminophosphate oxynitride samples (AlPON) were prepared by nitridation under ammonia of two different AlPO precursors. The nitridation method has been described elsewhere.[9,10] The citrate method was used for preparing the first AlPO precursor. In brief, it consists of mixing aqueous solutions of aluminum nitrate and monobasic ammonium phosphate of the same molarity at room temperature. An excess of citric acid was then added, and the mixture was kept overnight at room temperature under continous stirring. Water was then eliminated under vacuum at 313 K, and the resulting solid was oven-dried at 383 K and calcined at 773 K for 20 h. The second AlPO precursor was obtained by the sol−gel method developed by Kearby.[29]

Diffuse reflectance infrared Fourier transform spectra (DRIFTS) were collected with a Nicolet 510P spectrometer using a DTGS detector at 4 cm^{-1} resolution. X-ray photoelectron spectra (XPS) were obtained with a VG 100AX spectrometer using Mg Kα radiation.

4. Models

Usually, amorphous aluminophosphates (AlPO), the precursors of the AlPON catalyst systems, have been thought to present a local structure around aluminum and phosphorus similar to that present in $AlPO_4$, that is, [AlO_4] and [PO_4] tetrahedra sharing all four corners and resulting in the exclusive presence of Al−O−P links within the solid framework.[30] However, the presence of a strong *restrhalen* absorption in the DRIFTS spectra of the AlPO systems around 1300 cm^{-1} [13,31] that has to be ascribed to the existence of P═O bonds[32] together with recent theoretical studies of AlPO model systems,[21] assuming metaphosphate-like models, supports a new vision of the structure of amorphous aluminophosphates in which the solid is made of cyclic phosphate-like anions whose charges are compensated by aluminum cations. Also recently, the structures of crystalline $AlNa_3P_3O_9N$ solids have been described,[33] showing a metaphosphate-like structure with [PO_4] tetrahedra, [AlO_6] octahedra, and P−X−P links (X = O, N). Moreover, the existence of phosphazenes with a basic ring having P−N−P bonds is quite well-known. As most of the characterization studies have shown the presence in the AlPO systems of both tetrahedral phosphorus and aluminum cations, but also of penta- and hexacoordinated aluminum cations, the formation of alternating layers of some cyclic phosphate anions and γ-Al_2O_3 leading to a more or less ordered framework can be proposed.[21]

On the other hand, incorporation of nitrogen in the AlPO framework occurs without drastic modification of the textural properties of the precursors, indicating that, after nitridation, the basic local structure of aluminum and phosphorus is retained. Also, recent studies by X-ray photoelectron spectroscopy of galloaluminophosphate oxynitrides[34] shows that the oxygen/nitrogen substitution occurs preferentially around phosphorus rather than around aluminum atoms. In the latter study, the good correlation between surface and bulk nitrogen content suggests a homogeneous nitridation.

The choice of the model has, thus, to take into account the existence of phosphoryl groups and hence of P−O−P links within the solid, the P/Al ratios experimentally obtained, and the various possibilities of oxygen/nitrogen substitution. With this goal in mind, an eight-membered ring with a orthophosphate-like structure and a P/Al ratio equal to 1 was taken as starting point (see Figure 1). The different N/O ratios were modeled on a progressive substitution of ring O atoms by N atoms. This substitutional process results in compounds whose stoichiometry is represented by $Al_2P_2O_{4-x}(NH)_xO_8H_8$, where $0 \leq x \leq 4$. These stoichiometries allow the consideration of nitrogen contents in the range 0−20 wt %, similar to those found experimentally.

In these models the coordination polyhedra around phosphorus are always tetrahedral as indicated by ^{31}P MAS NMR data of AlPO systems[22] and also the coordination polyhedra around Al, since the IR spectra of AlPO systems show the existence of tetrahedral (as well as penta- and hexacoordinated) aluminum cations within the solid framework. When needed, the coordination of oxygen and nitrogen atoms was completed with hydrogen atoms (not shown in Figure 1), to simulate the next cation in the solid network and to have neutral molecular models. With respect to the starting model, corresponding to a pure AlPO solid, two different structures are possible with regard to the kind of M−O−M (M = P, Al) links within the ring. In one of these structures (series A), each phosphorus atom has the other phosphorus atom as a second neighbor, resulting in the existence of a P−O−P link on the structure, as well as two P−O−Al links and one Al−O−Al link. In the second structure (series

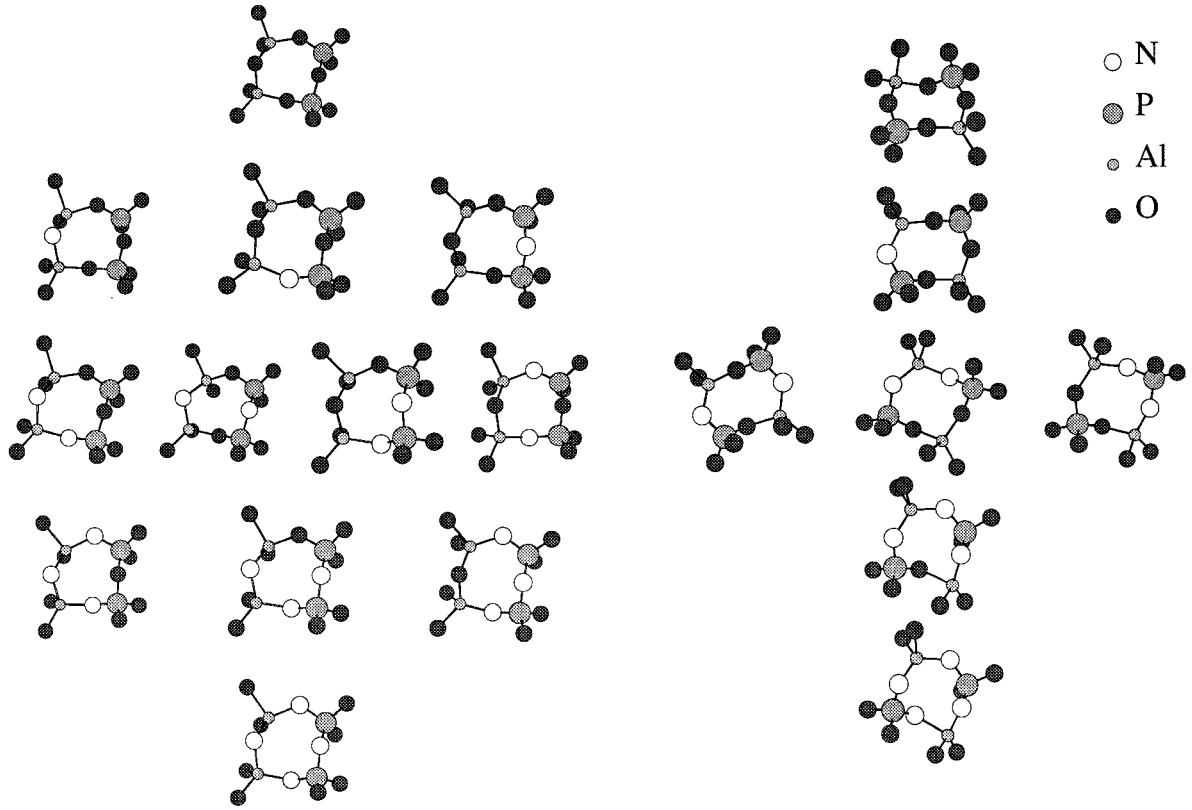

Figure 1. Molecular models of the AlPON solid system. Left side: A-series. Right side: B-series. Hydrogen atoms not shown. Models in a given row have the same N/O ratio, which increases from top to bottom.

TABLE 1: Selected Average Bond Distances (Å)

	N/O					
	0/4	1/3	2/2	3/1	4/0	average
A-Series						
P−OP	1.611	1.611	1.611	1.614		1.612 ± 0.022
P−OAl	1.539	1.540	1.542	1.545		1.541 ± 0.004
Al−OAl	1.696	1.695	1.697	1.697		1.696 ± 0.015
Al−OP	1.755	1.752	1.752	1.751		1.752 ± 0.009
P−NP		1.679	1.678	1.678	1.677	1.678 ± 0.02
P−NAl		1.639	1.641	1.634	1.639	1.638 ± 0.005
Al−NAl		1.791	1.793	1.795	1.798	1.794 ± 0.02
Al−NP		1.845	1.853	1.845	1.845	1.847 ± 0.011
B-Series						
P−OAl	1.549	1.549	1.552	1.548		1.550 ± 0.006
Al−OP	1.742	1.731	1.753	1.758		1.743 ± 0.012
P−NAl		1.625	1.633	1.634	1.633	1.633 ± 0.004
Al−NP		1.826	1.827	1.836	1.840	1.834 ± 0.009

B), phosphorus and aluminum atoms are alternating in the ring, resulting in the exclusive presence of P−O−Al links in the models. With the previous discussion about available structural experimental data on amorphous and crystalline AlPO systems in mind, series A models can be thought of as representative of amorphous AlPO(N) systems (presence of P−O−P links), while series B can be seen as a model for crystalline AlPO(N) solids (exclusive presence of P−O−Al links).

5. Results and Discussion

5.1. Geometrical Structure. A selected set of average optimized M−O (M = P, Al) bond distances is presented in Table 1. For different N/O ratios an average value has been obtained for all bond distances of the same type, and an average value for all N/O compositions is also shown.

The values presented in the table are shown to be basically independent of the N/O composition. Thus the P−OP bond distances (P−O with another P atom as a second neighbor of the O atom) range from 1.611 to 1.614 Å, with an average value of 1.612 ± 0.02 Å. The dispersion of the P−OAl distances, with an average value of 1.541 Å in the A-series, is even smaller (±0.004 Å). The same picture can be extracted from the examination of the Al−OM values: they show no significant variation with respect to the N/O ratio. The Al−O bond distances range from 1.695 to 1.697 Å and the Al−OP from 1.755 to 1.751 with an average value of 1.752 ± 0.009 Å. The most important differences appear when P−OP and P−OAl (or Al−OAl and Al−OP) bond distances are compared. As discussed elsewhere,[21] there is a large influence of the O-atom second neighbor on the P−O (or Al−O) bond distance. Thus, substitution of the P atom as a second neighbor of a P−O bond by the more electropositive Al atom decreases the bond distance by 0.071 Å, while the same substitution decreases the Al−O distance by 0.056 Å.

Similar findings are obtained by examination of the P−N and Al−N bond distances. They show no long-range effect of the N/O composition, and only the second neighbor of the N atom seems to affect the bond significantly. Again, when an Al atom is the second neighbor of the N atom, the M−N bond is shorter: the P−NAl bond distance (1.638 Å) is 0.04 Å shorter than the P−NP bond distance (1.678 Å); also the Al−NAl bond (1.794 Å) is shorter by 0.053 Å than the average of the Al−NP bond distances.

Comparison of P−O/P−N and Al−O/Al−N bond distances show that in all cases there is a small increase in M−X bond distance when oxygen is replaced by nitrogen. Thus, the P−NP average bond distance is 1.678 Å, i.e., 0.066 Å longer than the P−OP average bond distance (1.612 Å). The larger increase, 0.098 Å, occurs when the Al−OAl average bond distance (1.696 Å) is compared to Al−NAl (1.794 Å). These comparisons and the observed behavior of bond distances on increasing nitrogen

loading indicate that the N/O substitution does not influence the geometry of our model clusters to a significant extent, suggesting that the nitridation process will not significantly affect the solid framework of the AlPO precursor.

The geometrical parameters obtained for the B-series cluster models are nearly identical to the values obtained for the A-series, with differences too small to be significant.

The computed bond distances compare quite nicely with experimental values. In the monoclinic form of aluminum metaphosphate the phosphorus atoms are always in tetrahedral coordination, with P−O bond distances ranging from 1.468 to 1.593 Å.[35] Our computed P−OAl bond distance (1.541 Å in the A-series and 1.550 Å in the B-series) fits perfectly in this range, while the computed P−OP is slightly larger (1.612 Å); in any case, it is within error bars. In crystalline $AlPO_4$, where aluminum cations are in tetrahedral coordination,[36] the Al−O distances range from 1.606 to 1.740 Å, depending on the structural polymorph. The computed Al−OAl bond distances are within this range (average value 1.696 Å) and the Al−OP distances are a little longer, but only by ∼0.01 Å.

Compounds with phosphorus−nitrogen bonds are well-known[37] and are called phosphazenes, with many of them showing cyclic structures. The best known cyclophosphazenes are trimeric and tetrameric ones with structures similar to our molecular models of the amorphous AlPON system. The P−N bond distances in these systems lie in the 1.55−1.61 Å range, but these compounds present some π-bonding and, thus, these bond distances are shorter than the expected single bond P−N of 1.75−1.80 Å. Our computed P−N bond distances of 1.634 Å for P−NAl and 1.678 Å for P−NP are closer to the shorter experimental values, indicating that some π-bonding could exist. The agreement between our computed P−N bond distances and the experimental values has to be taken with caution. Although Hartree−Fock theory performs generally well for geometries, the experimental values, in this case, span a wide range, thus reducing the meaning of the comparison.

Compounds with Al−N bonds are relatively well-known and very often they present cyclic or cage structures;[38] polymers with Al−N backbones are also known. In these compounds the N atom is usually bonded tetrahedrally, with Al−N bond distances around 1.91−1.96 Å. Our computed Al−N bond distances are a little shorter than these values, ranging from 1.794 to 1.847 Å; however, the difference is small (∼0.1 Å) and can be explained by the reduced coordination of nitrogen in our molecular models.

5.2. Photoelectron Spectroscopy. The computed Koopman ionization potentials (IP) for different atomic orbitals are presented in Table 2, where aluminum and phosphorus 2s and 2p IPs are classed according to their first coordination shell. The absolute values of these IPs cannot be directly compared with experimental binding energies (BE), since the theoretical values do not incorporate the relaxation of the hole and thus are expected to be off the experimental values by 10−30 eV. Instead we will concentrate on examining trends by looking at the variation of these IP with composition and coordination polyhedra.

From the results presented in this table, two conclusions can be extracted: first, the IP for a given orbital and coordination polyhedra does not depend on the global N/O composition and, second, there is a shift in the IPs with composition at the first coordination shell. This shift is smaller for aluminum 2s and 2p orbitals whose IP are lowered only a maximum of 0.6 eV with increasing nitrogen content. The effect is more noticeable on phosphorus 2s and 2p orbitals that are shifted to lower values by around 1 eV on going from $[PO_4]$ to $[PO_2N_2]$ polyhedra.

TABLE 2: Computed Core Koopman IP/eV

		N/O				
		0/4	1/3	2/2	3/1	4/0
		A-Series				
Al_{2s}	AlO_4	133.4	133.3	133.2		
	AlO_3N		133.2	133.1	133.0	
	AlO_2N_2			132.9	132.9	132.8
Al_{2p}	AlO_4	87.6	87.5	87.4		
	AlO_3N		87.4	87.3	87.2	
	AlO_2N_2			87.4	87.1	87.0
P_{2s}	PO_4	207.2	207.1	207.1		
	PO_3N		206.9	206.8	206.7	
	PO_2N_2			206.3	206.3	206.2
P_{2p}	PO_4	150.0	149.9	149.8		
	PO_3N		149.6	149.5	149.4	
	PO_2N_2			149.1	149.1	149.0
O_{1s}	P−O−P	560.0	559.9	559.7	559.6	
	P−O−Al	558.9	558.8	558.5	558.5	
	Al−O−Al	557.6	557.5	557.5	557.5	
N_{1s}	P−N−P		423.2	423.1	423.1	423.1
	P−N−Al		422.2	422.1	421.9	421.9
	Al−N−Al		412.3	421.2	421.1	421.1
		B-Series				
Al_{2s}	AlO_4	133.4	133.2	133.2		
	AlO_3N		133.2	133.2	132.2	
	AlO_2N_2			133.0	133.1	131.9
Al_{2p}	AlO_4	87.8	87.7	87.6		
	AlO_3N		87.4	87.3	87.2	
	AlO_2N_2			87.2	87.3	87.2
P_{2s}	PO_4	207.1	206.9	206.9		
	PO_3N		206.9	206.7	206.5	
	PO_2N_2			206.3	206.3	206.2
P_{2p}	PO_4	150.1	149.9	149.9		
	PO_3N		149.6	149.4	149.3	
	PO_2N_2			149.1	149.1	149.0
O_{1s}	P−O−Al	559.2	559.1	558.9	558.7	
N_{1s}	P−N−Al		422.3	422.3	422.1	422.0

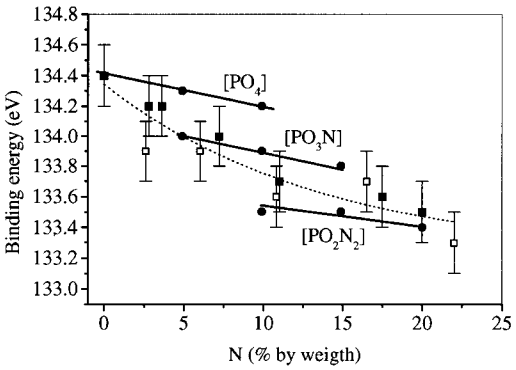

Figure 2. P_{2p} binding energies for the series of prepared catalysts. Theoretical Koopman IP values (circles); experimental data (squares); AlPO precursor obtained by the citrate method (filled squares); AlPO precursor obtained by Kearby's method (open squares).

Figure 2 shows the evolution of the P_{2p} binding energies as a function of the nitrogen content of the solids. It is clear from the figure that the precursor preparation method modifies the binding energy for the same nitrogen content. Yet, whatever the preparation method is, the experimental binding energies match quite well the calculated Koopman ionization potentials after subtraction of the estimated hole relaxation energy (15.6 eV).[21] Comparison of the experimental and theoretical values points out that for the highest nitrogen content experimentally obtained a $[PO_2N_2]$ polyhedra can be proposed, while for lower

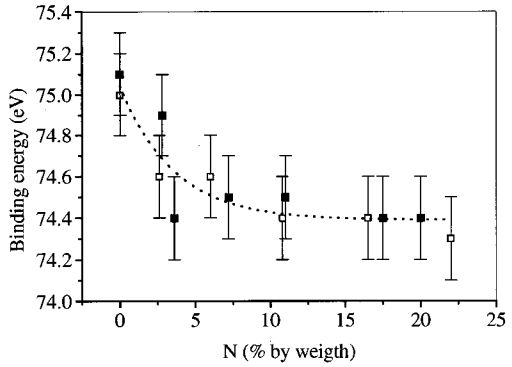

Figure 3. Al_{2p} binding energies for the series of prepared catalysts. Theoretical Koopman IP values (circles); experimental data (squares); AlPO precursor obtained by the citrate method (filled squares); AlPO precursor obtained by Kearby's method (open squares).

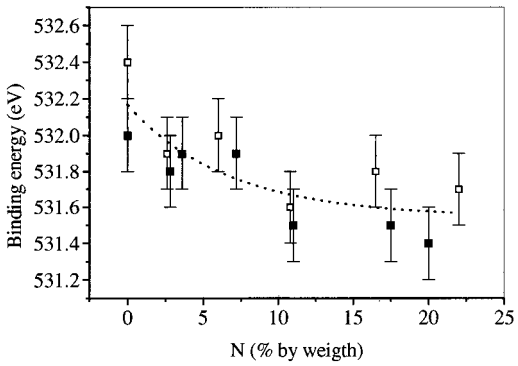

Figure 4. O_{1s} binding energies for the series of prepared catalysts. Theoretical Koopman IP values (circles); experimental data (squares); AlPO precursor obtained by the citrate method (filled squares); AlPO precursor obtained by Kearby's method (open squares).

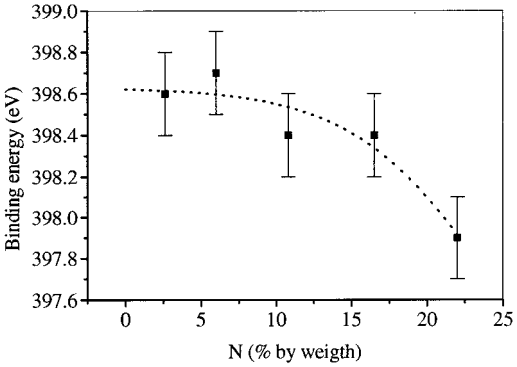

Figure 5. N_{1s} binding energies for the series of prepared catalysts. AlPO precursor obtained by the citrate method.

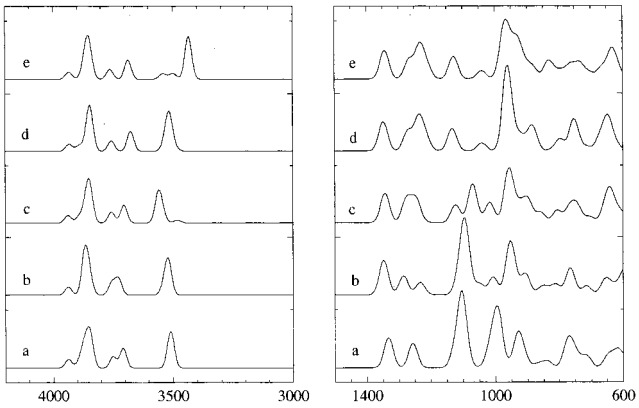

Figure 6. Simulated IR spectra for molecular models with different N/O compositions. (a) N/O = 0/4; (b) N/O = 1/3; (c) N/O = 2/2; (d) N/O = 3/1; (e) N/O = 4/0.

nitrogen contents a mixture of $[PO_{2-x}N_x]$ polyhedra is proposed. The precursor synthesis affects the nitridation mechanism, resulting in a different proportion of phosphorus coordination polyhedra for the same nitrogen content.

The variation of Al_{2p} binding energies as a function of nitrogen content, Figure 3, does not follow the same trend as phosphorus binding energies. After an initial decrease the Al_{2p} energy remains practically constant for all the nitrogen content range. It has to be taken into account that the selected models do not consider changes in the coordination polyhedra of aluminum, which in fact does occur on increasing nitrogen content.[18−20] Thus the initial decrease in binding energies might be tentatively ascribed to a modification of the aluminum coordination polyhedra rather than to the presence of nitrogen in the first coordination sphere of aluminum.

The values of oxygen and nitrogen 1s IPs also show a nice correlation with their first shell coordination polyhedra, and in this case the predicted shift on the IPs is larger. The O_{1s} IP is 557.5 eV when oxygen is bonded to two aluminum atoms, and increases by about 1.8 eV when an Al atom is substituted by a phosphorus atom and another 0.8 eV when the second aluminum is substituted. The same trend is observed when the N_{1s} IPs are examined. The IP increases by 0.9 eV when the first Al atom is substituted on the first coordination sphere of the nitrogen by a P atom and by another 1.0 eV when the second Al atom is substituted.

Figures 4 and 5 show the evolution of N_{1s} and O_{1s} binding energies as a function of the nitrogen content of the solids. To unequivocally explain the experimental data on the basis of the theoretical results cannot be straightforward in the case of the O_{1s} signal. The computed data in Table 2 accounts for the oxygen atoms in the metaphosphate-like ring. However, in the experimental spectra, the signals corresponding to these oxygens will overlap those arising from P═O, P−OH, and Al−OH bonds, giving rise to a broad band whose main position will depend on the dominant species present in the solid. Despite this fact there is a clear decrease in the O_{1s} signal upon increasing nitrogen content, which is clearly in agreement with the theoretical data. The strong initial decrease should be related to the fact that nitrogen enters the phosphorus coordination sphere preferentially; in this case the Al−O bonds, being predominant, show a lower binding energy than P−O bonds. This is also supported by the N_{1s} binding energy evolution. If nitrogen preferentially enters the phosphorus coordination sphere, N_{1s} binding energy should remain constant whatever the nitrogen content of the solids. The strong decrease for the highest nitrogen content should be related to the presence of Al−N bonds.

5.3. Infrared Spectroscopy. The computed vibrational spectra for the different molecular models with different nitrogen contents are shown in Figure 6. For each N/O composition where different substitutional isomers were possible, the isomer with the large number of N−P bonds was selected, to account for the experimentally observed selective replacement of oxygen bonded to P atoms.

The displayed spectra were calculated from the ab initio harmonic frequencies and intensities using a Gaussian function with a constant half-width to represent each peak. The peak height is computed from the calculated intensity. The computed harmonic frequencies were scaled by a factor of 0.92 to obtain

the displayed spectra. This procedure is well established and attempts to correct systematic errors in the computed RHF force field due to lack of electron correlation, limited size of basis set, and anharmonicity effects.

The main features of the computed vibrational spectra agree quite well with those observed in the experimental DRIFTS spectra. The O−H stretching modes were computed for the parent AlPO molecular model (Figure 6a) at 3710 and 3853 cm^{-1} for the hydroxyl groups bonded to P atoms and 3895 and 3941 cm^{-1} for the hydroxyls bonded to Al atoms. These values agree qualitatively with the two main peaks found in the experimental spectrum at 3673 and 3786 cm^{-1}, assigned to the O−H stretch of hydroxyl groups bonded to tetrahedral P and Al atoms, respectively. The intense peak seen in the simulated spectrum at 3516 cm^{-1} corresponds to the O−H stretch of one of the water molecules used to complete the coordination of the Al atoms which also presents a hydrogen bond to a neighboring hydroxyl group. This peak cannot be associated to any band in the experimental spectrum as any adsorbed water has been eliminated before recording the DRIFTS spectra of the samples. The limited agreement found between the computed and the experimental values is related to the limited size of the basis set used for the H atoms, which does not include polarization functions. The use of a 0.90 scaling factor is most appropriate in this case, closely matching the experimental data.

The N−H stretch appears in the computed IR spectra at 3542 ± 1 cm^{-1} for a P−NH−P bridging unit, at 3491 ± 2 and 3509 ± 2 cm^{-1} (antisymmetric and symmetric combinations) for a P−NH−Al bridging unit, and at 3508 cm^{-1} for a Al−NH−Al bridging unit. The computed values show almost no dependency on the global composition and are only a function of the coordination of the N atom. These calculated values allowed us to distinguish the coordination of the N atom in the framework, as the NH stretching of P−NH−P bridging unit is about 40 cm^{-1} larger than either the NH stretching for the P−NH−Al or the Al−NH−Al linkages. This larger value is also indicative of a stronger P−N−P bridging unit.

The observed peak in the experimental DRIFTS spectrum at about 1350 cm^{-1} corresponds to the stretch of P═O bonds, which are computed as two bands at 1337 and 1254 cm^{-1} (Figure 6b). The high-frequency band showed no noticeable shift with increasing nitrogen content in our molecular models. However, on increasing nitrogen content (N/O = 1/3), a new band developed in this region at 1289 cm^{-1} and mixed with the lower energy P═O stretch, displacing it to lower wavenumbers (1235 cm^{-1}). The analysis of the associated normal mode showed that this new band corresponds to a mixing of the N−H in-plane bending mode with the P═O stretch. The N−H bending mode frequency shows itself to be dependent, as the N−H stretch, on the two neighbors of the nitrogen atom, is shifted from ∼1280 cm^{-1} when the two neighbors are P atoms, to ∼1240 cm^{-1} when one P atom is substituted by an Al atom; and finally, it appears at about 980 cm^{-1}, obscured by other bands in the 1100−800 cm^{-1} region, when the two neighbors are Al atoms.

The intense band around 1350 cm^{-1} in the experimental spectra shifts toward a lower wavenumber on increasing nitrogen content (Figure 7). A large shift is observed for the higher nitrogen contents. As the P═O stretching mode is hardly dependent on the nitrogen content; it has to be assumed that the shift is the result of the combination of the P═O stretching mode with the N−H bending mode. As deduced from the XPS data, nitrogen enters the aluminum coordination sphere only for high nitrogen contents, the shift being larger in this case.

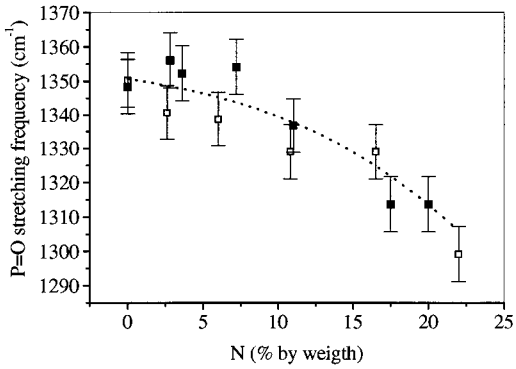

Figure 7. Evolution of P═O stretching band with N content of the solid. Experimental data. AlPO precursor obtained by the citrate method (filled squares); AlPO precursor obtained by Kearby's method (open squares).

The stretches of P−O and Al−O ring bonds appear in the computed spectrum of the parent AlPO model (N/O = 0/4, Figure 6b), as the main components of the intense bands centered at about 1100 and 1000 cm^{-1} (P−O) and 925 cm^{-1} (Al−O). These frequencies correspond closely to the observed peaks in the DRIFTS spectrum for P/Al = 1/1 around 1000−900 cm^{-1} and observed for $Al_4(P_4O_{12})_3$ at 1083, 1066, and 1029 cm^{-1}. Important changes are observed in this region on increasing nitrogen content. For N/O = 1/3 ratio, a new intense peak is computed at about 950 cm^{-1}, and intensity is lost on the band centered at 1000 cm^{-1}. Analysis of the associated vibrational modes reveal that the intense peak at 950 cm^{-1} corresponds mainly to P−N stretch modes and P−O stretch and Al−O stretch appear as shoulders of this band at 1000 (P−O) and 920 (Al−O) cm^{-1} ; the intense band that still appears centered at about 1100 cm^{-1} is associated to the stretch of P−O bonds. Substitution of bridge oxygen atoms by nitrogen atoms progressively produces an intensity shift toward lower wavenumbers. The P−O stretch band at 1000 cm^{-1} loses intensity for N/O = 2/2 and is definitively lost for N/O = 3/1. Concurrently, the P−N stretch band at 950 cm^{-1} gains intensity as more P−N bonds exist in the framework.

5.4. Thermodynamic Stability. One of the key issues in this research is to understand, at least from a thermodynamic viewpoint, the extent and nature of N/O substitution and to evaluate the relative stability of [Al−NH−Al], [Al−NH−P], and [P−NH−P] bridging units. In Table 3 we present the computed reaction energies for the generic process

$$\mathrm{AlPO} + n\mathrm{NH_3} \rightarrow \mathrm{AlPO(NH)}_n + n\mathrm{H_2O}$$

that represents the substitution of n bridging oxygens [M−O-M′] by NH-bridging groups [M−NH−M′] in both A- and B-series molecular models of the AlPO framework. Given the theoretical level of calculation and the limited size of the models, these results are to be taken as qualitative but indicative of generic trends in the energetics of the substitution process.

The values obtained for the four substitutions in the B-series are quite similar, increasing only slightly, from 22.0 to 27.2 kcal·mol^{-1} with increasing nitrogen content. These results indicate the high stability of [Al−O−P] bridges and that the progressive nitrogen loading has little effect on nearby [Al−O−P] bridges.

More interesting yet are the results obtained in the A-series, where different [M−O−M′] bridges are available for substitution. The first substitution can occur at three different positions, giving place to [P−NH−P], [P−NH−Al], and [Al−NH−Al] bridges. The energetic results presented show clearly that

TABLE 3: Computed RHF Reaction Energies for the Generic Process

$$AlPO + nNH_3 \rightarrow AlPO(NH)_n + nH_2O$$

			ΔE/kcal·mol^{-1}	
N/O	series	link(s)	*a*	*b*
1/3	A	[P−NH−P]	13.5	
		[P−NH−Al]	27.9	
		[Al−NH−Al]	31.5	
	B	[P−NH−Al]	22.0	
2/2	A	[P−NH−P] + [P−NH−Al]	40.1	26.6
		[P−NH−P] + [Al−NH−Al]	45.2	31.7
	B	2[P−NH−Al]	44.7	22.7
3/1	A	[P−NH−P] + 2[P−NH−Al]	72.5	32.4
		[P−NH−P] + [P−NH−Al] + [Al−NH−Al]	79.0	38.9
	B	3[P−NH−Al]	69.2	24.5
4/0	A	[P−NH−P] + 2[P−NH−Al] + [Al−NH−Al]	98.7	26.2
	B	4[P−NH−Al]	96.9	27.7

[a] Total reaction energy at this step. [b] Reaction energy relative to previous step.

substitution at a [P−O−P] bridge is the most favorable process, this being endothermic by 13.5 kcal·mol^{-1} only, whereas nitridation at a [P−O−Al] or [Al−O−Al] bridges are endothermic by 27.9 or 31.5 kcal·mol^{-1}, respectively. The second substitution can take place now at a [P−O−Al] or at a [Al−O−Al] bridge, and the computed energies for these substitution are similar to those computed for the initial substitution at the same places: 26.6 and 31.7 kcal·mol^{-1}, respectively. Further nitridation gives similar results, indicating that, as deduced from the results obtained for the A-series, nitridation has little effect on nearby [M−O−M′] bridges in the framework.

Thus, from a thermodynamic viewpoint, preferential substitution should occur initially at [P−NH−P] bridges at relatively low temperatures and only at higher temperatures should [Al−NH−P] and/or [Al−NH−Al] groups be formed. These results point out how the structural difference existing between amorphous AlPO (existence of [P−O−P] links) and crystalline AlPO (exclusive presence of [P−O−Al] bridges) affects the nitridation process. While in amorphous AlPO, initial nitridation at [P−O−P] is relatively easy and should happen at moderate temperatures, in crystalline AlPO systems, where only [Al−O−P] links exist, nitridation of these links is a more energetically demanding process requiring a higher reaction temperature.

6. Concluding Remarks

Ab initio RHF molecular orbital calculations have been performed on metaphosphate-like model structures used to obtain structural and energetic information on aluminophosphate oxynitride (AlPON) systems. The observed trends in computed photoelectron energies, frequencies of the vibrational modes, and thermodynamic stability are compared with experimental spectroscopic data.

The short-range order in the amorphous solids may be deduced from the experimental data in light of the theoretical calculations. From the XPS data, it can be concluded that first nitrogen enters the phosphorus coordination sphere, resulting in the formation step by step of $[PO_3N]$ and $[PO_2N_2]$ polyhedra that coexist with $[PO_4]$ ones, their relative proportion depending on the total nitrogen content of the sample. The evolution of O_{1s} and N_{1s} binding energies suggests that on nitriding the samples the formation of P−N−P bonds occurs, which is also supported by their relative thermodynamic stability with respect to P−N−Al and Al−N−Al bonds. If the nitrogen content increases over a certain value (typically 15−20 wt %), the formation of P−N−Al bonds occurs, which may indicate that metaphosphate-like rings are linked to each other through aluminum bridges. On reaching the nitridation limit, the formation of P−N−Al bonds is required, but as the thermodynamic stability of these bonds is much lower than that of P−N−P bonds the nitridation process is not allowed to continue.

On the basis of both experimental and ab initio SCF calculations, it can be concluded that the amorphous solids are formed by P−X−P (X = O, N) rings connected to each other by aluminum atoms. On the basis of the thermodynamic stability of the different bonds, nitrogen enters preferentially the phosphorus coordination sphere.

Acknowledgment. The authors thank A. Massinon and R. Conanec for sample preparation and the Centro Informático Científico de Andalucía (CICA) for computational facilities. Financial support has been provided by the Spanish DGICyT (Project No. PB98-1125 and MAT94-0434-C03-02).

References and Notes

(1) Sauer, J. *Chem. Rev.* **1989**, 89, 199.
(2) Babu, G. P.; Ganguli, P.; Metcalfe, K.; Rockliffe, J. W.; Smith, E. G. *J. Mater. Chem.* **1994**, *4*, 331.
(3) Campelo, J. M.; García, A.; Luna, D.; Marinas, J. M.; Romero, A. A.; Navío, J. A.; Macías, M. M. *J. Chem. Soc., Faraday Trans.* **1994**, *90*, 2265.
(4) Campelo, J. M.; García, A.; Luna, D.; Marinas, J. M. *J. Catal.* **1986**, *102*, 299.
(5) Rebenstorf, B.; Lindbland, T.; Andersson, S. L. *J. Catal.* **1991**, *128*, 293.
(6) Andersson, S. L. *Appl. Catal. A* **1989**, *112*, 209.
(7) Kuo, P. S.; Yang, B. N. *J. Catal.* **1989**, *117*, 301.
(8) Campelo, J. M.; García, A.; Luna, D.; Marinas, J. M. *J. Catal.* **1988**, *113*, 172.
(9) Marchand, R.; Conanec, R.; Laurent, Y.; Bastians, P.; Grange, P.; Gandía-Pascual, L. M.; Fernández Sanz, J.; Odriozola, J. A. Patent No. Fr9401081.
(10) Grange, P.; Bastians, P.; Conanec, R.; Marchand, R.; Laurent, Y.; Gandía, L.; Montes, M.; Fernández Sanz, J.; Odriozola, J. A. *Stud. Surf. Sci. Catal.* **1995**, *91*, 381.
(11) Grange, P.; Bastians, R.; Conanec, R.; Marchand, R.; Laurent, Y. *Appl. Catal. A* **1994**, *114*, L191.
(12) Massinon, A.; Odriozola, J. A.; Bastians, Ph.; Conanec, R.; Marchand, R.; Laurent, Y.; Grange, P. *Appl. Catal. A* **1996**, *137*, 9.
(13) Benítez, J. J.; Odriozola, J. A.; Marchand, R.; Laurent, Y.; Grange, P. *J. Chem. Soc. Faraday Trans.* **1995**, *91*, 4477.
(14) Gandía, L. M.; Malm, R.; Marchand, R.; Conanec, R.; Laurent, Y.; Montes, M. *Appl. Catal. A* **1994**, *114*, L1.
(15) Guéguen, E.; Delsarte, S.; Peltier, V.; Conanec, R.; Marchand, R.; Laurent, Y.; Grange, P. *J. Eur. Ceram. Soc.* **1997**, *17*, 2007.
(16) Centeno, M. A.; Grange, P. *J. Phys. Chem. B* **1999**, *103*, 2431.
(17) Centeno, M. A.; Debois, M.; Grange, P. *J. Phys. Chem. B* **1998**, *102*, 6835.
(18) Benítez, J. J.; Díaz, A.; Laurent, Y.; Odriozola, J. A. *Catal. Lett.* **1998**, *54*, 159.
(19) Díaz, A.; Benítez, J. J.; Laurent, Y.; Odriozola, J. A. *J. Non-Cryst. Solids* **1998**, *238*, 163.
(20) Benítez, J. J.; Díaz, A.; Laurent, Y.; Grange, P.; Odriozola, J. A. *Z. Phys. Chem.* **1997**, *202*, 21.
(21) Márquez, A.; Oviedo, J.; Fernández Sanz, J.; Benítez, J. J.; Odriozola, J. A. *J. Phys. Chem. B* **1997**, *101*, 9510.
(22) Conanec, R. Ph. D. Thesis, University of Rennes I, 1994.
(23) Pulay, P.; Fogarasi, G.; Pang, F.; Boggs, J. E. *J. Am. Chem. Soc.* **1979**, *101*, 2550.
(24) Fogarasi, G.; Zhou, X.; Taylor, P. W.; Pulay, P. *J. Am. Chem. Soc.* **1992**, *114*, 8191.
(25) Komornicki, A.; McIver, J. W. *J. Chem. Phys.* **1979**, *70*, 2014.
(26) Dupuis, M.; Johnston, F.; Márquez, A. HONDO 8.5 from ChemStation; IBM Corp.: Neighborhood Road, Kingston, NY, 1994.
(27) Dupuis, M.; Chin, S.; Márquez, A. Modern Tools for Including Electron Correlation in Electronic Structure Studies: HONDO and ChemStation. In *Relativistic and Electron Correlation Effects in Molecules and Solids*; Malli, G. L. Ed.; NATO ASI Series; Plenum Press: New York, 1994.

(28) Márquez, A.; Oviedo, J., Fernández Sanz, J.; Dupuis, M. *J. Comput. Chem.* **1997**, *18*, 159.
(29) Kearby, K. *Proc. 2nd Int. Congr. Catal.*; Technip: Paris, 1961; p 2567.
(30) Muller, O.; Roy, R. *The Major Ternary Structural Families*; Springer-Verlag: New York, 1974.
(31) Benítez, J. J.; Centeno, M. A.; Odriozola, J. A.; Conanec, R.; Marchand, R.; Laurent, Y. *Catal. Lett.* **1995**, *35*, 379.
(32) Corbridge, D. E. C. In *Topics in Phosphorous Chemistry*; Grayson, M., Griffith, E.J., Eds; John Wiley and Sons: New York, 1989; Vol. 6, p 235.
(33) Conanec, R.; L'Haridon, P.; Feldmann, W.; Marchand, R. Laurent, Y. *Eur. J. Solid State Inorg. Chem.* **1994**, *31*, 13.
(34) Delsarte, S.; Peltier, V.; Laurent, Y.; Grange, P. *J. Eur. Ceram. Soc.* **1998**, *18*, 1287.
(35) van de Meer, H. *Acta Crystallogr. B* **1976**, *32*, 2423.
(36) Pauling, L.; Sherman, J. *Z. Krystallogr.* **1937**, *96*, 481.
(37) Cotton, F. A.; Wilkinson, G. *Advanced Inorganic Chemistry*, 5th ed; Wiley: New York, 1988.
(38) Wells, A. F. *Structural Inorganic Chemistry*, 5th ed.; Clarendon Press: Oxford, 1984.